



Trends in
**Applied Sciences
Research**

ISSN 1819-3579



Academic
Journals Inc.

www.academicjournals.com

Effectiveness of Kriging Interpolation Technique for Estimating Permeability Distribution of a Field

O. Anomohanran and U. Chapele

Department of Physics, Delta State University, Abraka, Nigeria

*Corresponding Author: O. Anomohanran, Department of Physics, Delta State University, Abraka, Nigeria
Tel: +2348039488655*

ABSTRACT

This study seeks to investigate the effectiveness of using the kriging interpolation technique in estimating the permeability distribution of a field. In carrying out this study, the permeability of three sand layers each of 39 wells in a field were obtained from the record of porosity and water saturation using the Tixier and Timur empirical models. The permeability of the three layers was also determined experimentally from core samples in the laboratory. Result shows strong correlation between core and derived permeability. The derived permeability values were used as input data in the kriging interpolation. Result shows that the kriged permeability for layer one ranges from 0.81 to 3.98 D for Tixier empirical model while the Timur model yielded a permeability range of 0.97 to 3.80 D. For the second layer, the Tixier model yielded a permeability range of 0.40 to 3.69 D while that of Timur gave a range of 0.38 to 3.59 D. For the third layer, the Tixier model gave a range of 0.20 to 0.95 D while the Timur model gave a range of 0.30 to 1.10 D. This study has revealed that there is consistency in the values of the permeability distribution obtained for both the Tixier and Timur models. The study also shows that there is decrease of permeability with increase in depth. The study has shown that the kriging algorithm can be used effectively in generating a two dimensional permeability distribution that is reliable with error ranging from 0.6 to 2.4%.

Key words: Kriging, permeability, Tixier, Timur, porosity, water saturation

INTRODUCTION

The permeability of a rock or soil is defined as its ability to transmit fluid through its pores or voids. Permeability is a property of the soil which is very useful to researchers interested in investigating the characteristics of the various soil layers in geophysical exploration of the subsurface (Alipour, 2007; Todd, 2004). Permeability is a parameter which determines whether a well should be completed and brought on stream or not. An effective management of reservoirs can be carried out only if the rock properties such as porosity, water saturation and permeability are well known (Mohaghegh *et al.*, 1995; Aigbedion, 2007; Merdhah and Yassin, 2009). Of all these properties, permeability has drawn much attention because of the complexity involved in predicting it accurately (Balan *et al.*, 1995; Tang and Cheng, 1996). Nevertheless, a lot of improvements have been successfully recorded empirically in the determination of permeability (Bloch, 1991; Yamamoto, 2003; Fernando, 2008).

Once the properties of the rock are known, it is possible to determine the permeability distribution using records from wells. In doing so, zones or layers which are found to be similar in properties can be correlated together in a bid to determine the distribution (Balan *et al.*, 1995; Mohaghegh *et al.*, 1997; Qobi *et al.*, 2001).

It is now very possible to draw up relationships between porosity, water saturation and permeability through the means of empirical models (Kapadia and Menzie, 1985). The records of well log are used to estimate effective porosity and irreducible water saturation which becomes the source data in empirically developed models (Orodu *et al.*, 2009).

Some empirical models based on the relationship between permeability, porosity and irreducible water saturation are the Tixier and the Timur approach. The Tixier model for determining permeability is expressed as:

$$K^{\frac{1}{2}} = 250 \frac{\phi^3}{S_{wi}} \quad (1)$$

On the other hand, the Timur model for the estimation of permeability is expressed as:

$$K = \frac{0.136\phi^{4.4}}{S_{wi}^2} \quad (2)$$

where, ϕ stands for the rock porosity and S_{wi} is the irreducible water saturation (Balan *et al.*, 1995; Mohaghegh *et al.*, 1995).

Kriging is a geostatistical technique used in formulating unbiased estimates of regionalized variables at some locations (Bayraktar and Turalioglu, 2005; Emery, 2005; Balasundram *et al.*, 2007, 2008). Kriging can be applied to estimate the value of a variable at a particular point or to estimate the average value of a block. It is known by the acronym "BLUE" also known as the "Best Linear Unbiased Estimator" (Negreiros *et al.*, 2010). Kriging interpolation models have shown success in its application in many areas of research. These include predicting groundwater level, soil salinity, soil fertility property and areal storm pattern analysis (Yasrebi *et al.*, 2008; Sokouti and Mahdian, 2009; Rabah *et al.*, 2011). Kriging when applied to research data gives values which best represent the distribution of the original data (Mohaghegh *et al.*, 1997; NIH, 1998).

If we consider a situation in which a property is measured at a number of points, x_i , within a region to give values of $Z(x_i)$, where $i = 1, 2, 3, \dots, N$, the value of the property at any place x_0 can be estimated. The place might be a point or an area of the same size and shape or a block. Kriging computes the best linear unbiased estimate based on a stochastic model of the spatial dependence (Tonkin and Larson, 2002).

In the simplified kriging equation, the kriged estimate is given as:

$$Z_x^* = \sum w_i Z(x_i) \quad (3)$$

where, w_i is the weight assigned to the sample Z at location x_i (Largueche, 2006; Balasundram *et al.*, 2007; Akbari *et al.*, 2009).

The kriging weights are unique in the sense that they eradicate the effect of bias towards input sample values (Vann *et al.*, 2003).

This study is therefore aimed at investigating the effectiveness of estimating the permeability distribution of a field using the kriging interpolation technique. This is carried out by employing the Tixier and the Timur empirical models of permeability distribution.

MATERIALS AND METHODS

Core samples of three sand layers each of thirty nine wells from a field were subjected experimentally to permeability test in the laboratory. The porosity ϕ for the three layers was obtained from the sonic and density logs of the wells while the resistivity log was used to compute the water saturation S_w . The porosity and water saturation were used to derive the permeability for the three different sand zones using the Tixier and the Timur empirical relation as stated in Eq. 1 and 2. The values obtained were compared with the core permeability values obtained from laboratory analysis. Since, there was strong correlation between the core permeability and the Tixier and Timur's derived permeability, the derived permeability were used as input data in the kriging process to derive the permeability distribution of the field.

The study area was divided into a square grid and permeability was estimated at each of the grid nodes using the Tixier and Timur derived data as the respective variables. Since we have thirty nine wells in the field, it follows that we have thirty nine equations corresponding to these points which represent the locations of the wells. There is also an equation that constrains the sum of the weighting coefficients to be one. The sum of squares of the differences between the core permeability and estimated values were obtained. This leads to the universal kriging system which in matrix form is expressed as Eq. 4 (Negreiros *et al.*, 2010). The result of the kriging operation is a 40x40 matrix and a 1x40 matrix. The 40x40 matrix was inverted in this study and its product multiplied with the 1x40 matrix to obtain the weighing coefficients for estimating the permeability at each grid location. This technique is applied to the three sand zones in the field of study:

$$\begin{bmatrix} X_{11} & X_{12} & \dots & X_{1n} & 1 \\ X_{21} & X_{22} & \dots & X_{2n} & 1 \\ X_{31} & X_{32} & \dots & X_{3n} & 1 \\ " & " & \dots & " & " \\ " & " & \dots & " & " \\ X_{n1} & X_{n2} & \dots & X_{nn} & 1 \\ 1 & 1 & 1 & 0 & 0 \end{bmatrix}^{-1} \begin{bmatrix} x_1 z_1 \\ x_2 z_2 \\ x_3 z_3 \\ " \\ " \\ x_n z_n \\ y \end{bmatrix} = \begin{bmatrix} a_1 \\ a_2 \\ a_3 \\ " \\ " \\ a_n \\ 1 \end{bmatrix} \tag{4}$$

The values of the coefficients obtained by solving Eq. 4 are substituted into Eq. 5 to yield the permeability at successive grid points:

$$Z = a_1 X_1 + a_2 X_2 + a_3 X_3 + \dots + a_n X_n \tag{5}$$

The values of permeability so obtained are then posted to the grid points and were contoured to show the permeability distribution. The error associated with the kriged values was determined by calculating the standard deviation between the kriged permeability value and the true permeability value.

RESULTS

The record of the porosity and water saturation obtained for this study as well as the derived permeability using the Tixier and the Timur models are as shown in Table 1. These were records computed from three sand zones located at a depth of between 7995 to 8010 feet for zone 1, 8100 to 8130 feet for zone 2 and 8280 to 8300 feet for zone 3. Because of the strong correlation between the measured and the derived data, the log derived permeability was used in obtaining the distribution for the reason that they can from the analysis, accurately and consistently determine

Table 1: Table showing porosity, water saturations, Tixier and Timur's derived permeability for the three sand zones

Sand zone 1				Sand zone 2				Sand zone 3			
PHI	SW	K. Tixier	K. Timur	PHI	SW	K. Tixier	K. Timur	PHI	SW	K. Tixier	K. Timur
0.30	0.16	2793	2664	0.28	0.27	701	757	0.22	0.28	224	348
0.29	0.17	1810	1857	0.26	0.33	308	393	0.24	0.20	404	556
0.26	0.14	725	876	0.24	0.40	229	311	0.26	0.10	798	963
0.30	0.14	2463	2399	0.24	0.52	261	346	0.23	0.29	316	457
0.30	0.11	2463	2399	0.29	0.41	1293	1237	0.27	0.15	1076	1227
0.32	0.19	4479	3959	0.27	0.36	502	580	0.25	0.17	545	708
0.29	0.24	1823	1868	0.25	0.37	246	330	0.24	0.18	451	608
0.30	0.14	2579	2492	0.23	0.49	161	236	0.24	0.27	378	528
0.30	0.15	2399	2347	0.27	0.39	351	436	0.23	0.26	348	494
0.27	0.17	927	1069	0.25	0.39	296	381	0.26	0.11	747	913
0.31	0.14	3366	3114	0.29	0.40	913	935	0.25	0.18	71	837
0.30	0.14	3652	2551	0.23	0.49	157	231	0.23	0.28	358	505
0.28	0.21	1236	1355	0.25	0.38	247	331	0.25	0.14	588	753
0.27	0.17	1033	1169	0.27	0.40	535	610	0.26	0.10	828	993
0.30	0.19	4363	3873	0.27	0.36	537	612	0.25	0.17	552	716
0.31	0.15	2466	2400	0.23	0.49	165	240	0.23	0.29	291	428
0.30	0.13	3015	2840	0.27	0.45	679	478	0.26	0.17	820	985
0.30	0.16	2166	2155	0.23	0.49	163	238	0.26	0.12	781	946
0.30	0.14	2666	2562	0.25	0.41	540	615	0.24	0.27	402	554
0.27	0.18	1111	1241	0.27	0.40	551	624	0.26	0.10	839	1003
0.31	0.14	3165	2957	0.29	0.39	1097	1084	0.26	0.18	687	853
0.30	0.11	2508	2435	0.30	0.40	1182	1151	0.27	0.16	935	1095
0.30	0.18	2252	2226	0.25	0.41	539	614	0.23	0.27	282	417
0.30	0.14	2635	2537	0.23	0.49	156	230	0.23	0.28	347	493
0.26	0.14	729	879	0.24	0.40	228	310	0.26	0.10	798	963
0.30	0.16	2710	2597	0.28	0.28	638	702	0.22	0.27	250	380
0.30	0.16	2708	2596	0.28	0.28	637	702	0.22	0.27	249	378
0.31	0.14	3166	2958	0.29	0.39	1088	1077	0.25	0.18	685	851
0.29	0.17	1931	1959	0.26	0.33	326	411	0.24	0.20	387	537
0.32	0.19	4371	3878	0.27	0.36	536	611	0.25	0.17	550	713
0.31	0.14	3264	3035	0.29	0.39	1001	1007	0.25	0.18	672	838
0.30	0.18	2252	2226	0.25	0.41	538	613	0.23	0.27	282	417
0.30	0.14	2462	2397	0.24	0.52	228	310	0.23	0.29	312	452
0.30	0.13	2598	2508	0.21	0.53	89	148	0.24	0.26	407	559
0.32	0.17	3927	3544	0.28	0.38	753	802	0.25	0.17	599	764
0.32	0.17	3930	3547	0.28	0.38	750	799	0.25	0.17	599	763
0.32	0.17	3935	3550	0.28	0.38	747	796	0.25	0.17	598	763
0.31	0.15	3478	3201	0.28	0.36	780	824	0.25	0.19	572	736
0.31	0.15	3534	3243	0.28	0.36	748	798	0.25	0.19	547	710

K: Permeability

permeability. The values obtained were interpolated at the nodes of square grid. The contour maps of the permeability distribution so obtained are presented as Fig. 1 to 6. The result of this interpolation for the Tixier method for zones 1, 2 and 3 is as shown in Fig. 1, 3 and 5, respectively while the result for the Timur interpolation for the three zones are as shown in Fig. 2, 4 and 6.

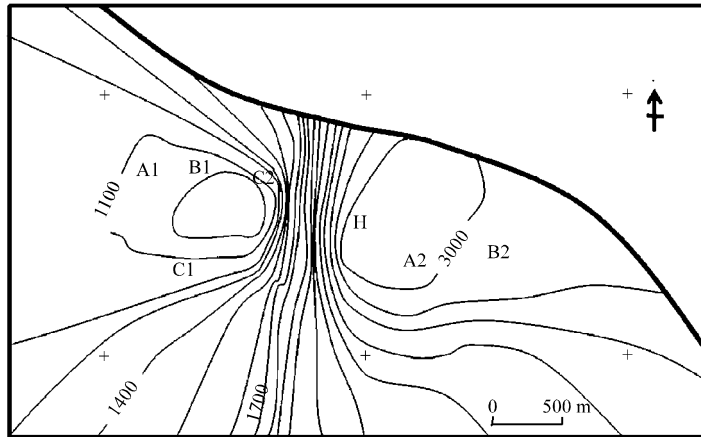


Fig. 1: Permeability contours in mD using Tixier's equation for zone 1

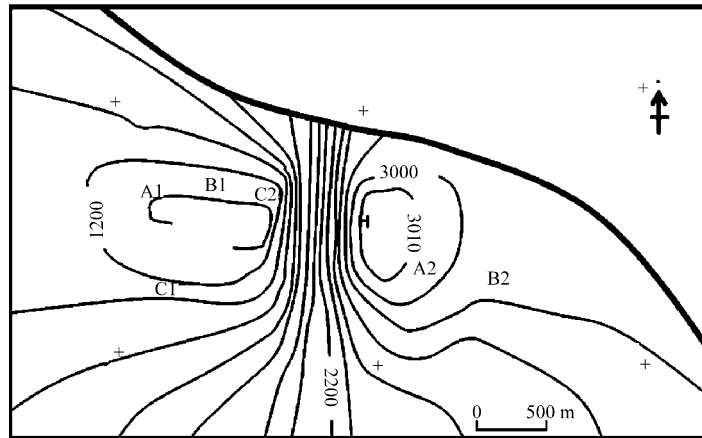


Fig. 2: Permeability contours in mD using Timur's equation for zone 1

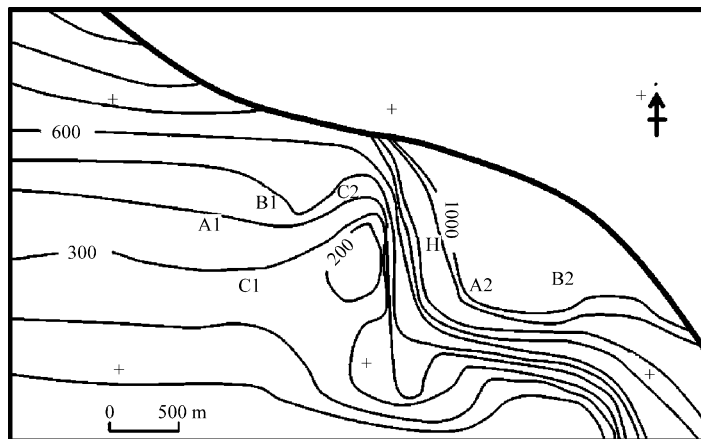


Fig. 3: Permeability contours in mD using Tixier's equation for zone 2

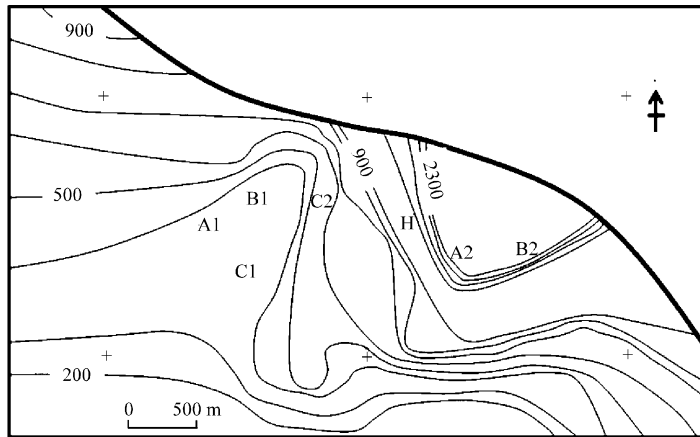


Fig. 4: Permeability contours in mD using Timur's equation for zone 2

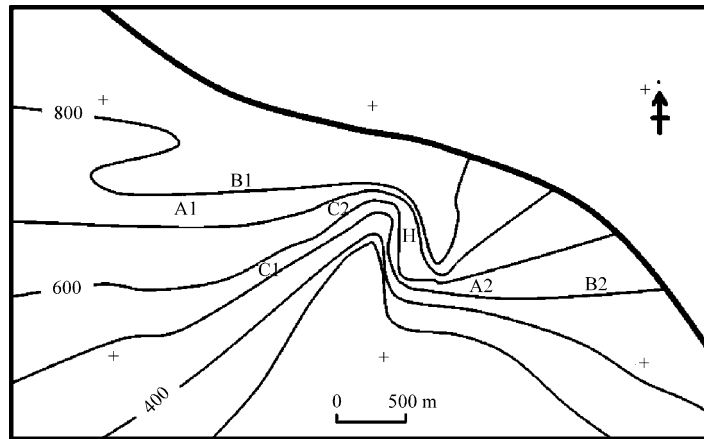


Fig. 5: Permeability contours in mD using Tixier's equation for zone 3

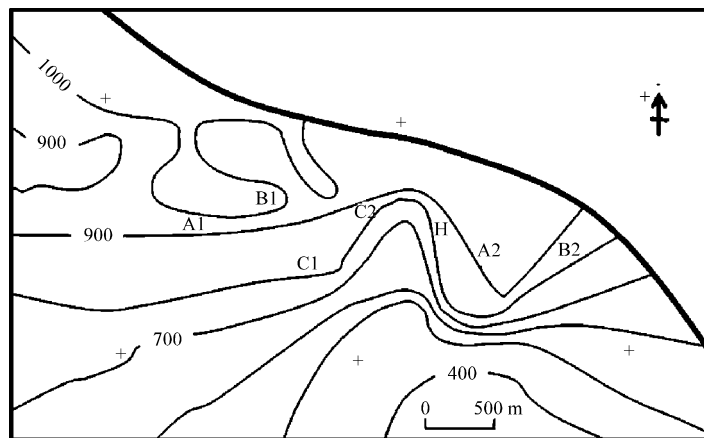


Fig. 6: Permeability contours in mD using Timur's equation for zone 3

DISCUSSION

The result in Fig. 1 shows that the permeability for zone 1 increases from well B towards well H and increased as we move northward. This trend changes with a decrease from that point as we move downward. This stress leads to a reduction in porosity and thus a decrease in permeability. This situation also plays out in Fig. 2 for the Timur's permeability distribution. The kriged permeability ranged from 0.81-3.98 D for the Tixier model and 0.97-3.80 D for the Timur model.

The permeability distribution as shown in both Fig. 3 and 4 for zone 2 lies side by side in a northwest trend close to the fault. Large spacing occurs between the contours as we move southwards. The permeability on the average for this sand zone is slightly lower than what was obtained for zone 1. It ranged from 0.40-3.64 D for the Tixier model and 0.38-3.59 for the Timur model.

For zone 3, the permeability ranged from 0.2-0.95 D for the Tixier model and 0.3-1.1 D for the Timur model as is shown in Fig. 5 and 6, respectively. These values are lower than what was obtained for zone 2 indicating a decrease in permeability with increase in depth. This finding is in support of the study of Saar and Manga (2004) that permeability is depth dependence. It is also in agreement with the findings of Morrow *et al.* (1994) that the values of permeability are based on rock type and depth. Figure 5 and 6 shows the permeability zone running from west to north east. Both contours show an increase in permeability northwards. The error obtained from each grid point for the various zones ranges from 0.6-2.4% which confirm reliability of the method used (Anomohanran, 2004). Result has also shown that the two models produced a similar trend for the three layers mapped in this study showing that the kriging method used in the permeability distribution is suitable for estimating the permeability at any point in the field.

This study has shown that there is strong correlation between the core permeability and the derived permeability using the Tixier and the Timur models. This view supports the findings by Shang *et al.* (2003) that there is a better correlation between measured and estimated permeability.

CONCLUSION

In this study, geostatistical techniques using the Tixier and Timur equations were applied to the field data to determine the permeability. The permeability distributions derived from the Tixier and Timur models produced a similar pattern in contours for each of the three sand zones investigated. The contours show areas of equal permeability and can be used in predicting the best direction and position to drill a well. This study has also shown that there is an observed decrease in permeability with increase depth. The results of this study emphasize that permeability have spatial dependence and that understanding such structure may provide insight into the permeability of the field.

REFERENCES

- Aigbedion, 2007. A case study of permeability modeling and reservoir performance in the absence of core data in the Niger Delta, Nigeria. *J. Applied Sci.*, 7: 772-776.
- Akbari, A., A. Abu Samah and F. Othman, 2009. Effect of pixel size on the areal storm pattern analysis using kriging. *J. Applied Sci.*, 9: 3707-3714.
- Alipour, S., 2007. Classification of soils based on double ring measured permeability in Zarrineh-Roud delta, Western Azarbayegan, Iran. *Pak. J. Biol. Sci.*, 10: 2522-2534.
- Anomohanran, O., 2004. The use of third degree polynomial for accurate conversion of seismic time to depth and vice versa. *J. Nig. Assoc. Math. Phys.*, 8: 241-246.

- Balan, B., S. Mohaghegh and S. Ameri, 1995. State-of-the-art in permeability determination from well log data: Part I-a comparative study, model development. Proceedings of the SPE Eastern Regional Conference and Exhibition, September 17-21, 1995, Morgantown, West Virginia, USA., pp: 1-10.
- Balasundram, S.K., D.J. Mulla and P.C. Robert, 2007. Spatial data calibration for site-specific phosphorus management. *Int. J. Agric. Res.*, 2: 888-889.
- Balasundram, S.K., M.H.A. Husni and O.H. Ahmed, 2008. Application of geostatistical tools to quantify spatial variability of selected soil chemical properties from a cultivated tropical peat. *J. Agron.*, 7: 82-87.
- Bayraktar, H. and F.S. Turalioglu, 2005. A Kriging-based approach for locating a sampling site: In the assessment of air quality. *Stochastic Environ. Res. Risk Assess.*, 19: 301-305.
- Bloch, S., 1991. Empirical prediction of porosity and permeability in sandstones. *AAPG Bull.*, 75: 1145-1160.
- Emery, X., 2005. Simple and ordinary multigaussian kriging for estimating recoverable reserves. *Math. Geol.*, 37: 295-319.
- Fernando, J., 2008. Determination of coefficient of permeability from soil percolation test. Proceedings of the 12th International Conference of IACMAG, October 1-6, 2008, Goa, India, pp: 1324-1331.
- Kapadia, S.P. and D.E. Menzie, 1985. Determination of permeability variation factor V from log analysis. Proceedings of the SPE Annual Technical Conference and Exhibition, September 22-26, 1985, Las Vegas, Nevada, pp: 1-12.
- Largueche, F.Z.B., 2006. Estimating soil contamination with kriging interpolation method. *Am. J. Applied Sci.*, 3: 1894-1898.
- Merdhah, A.B.B. and A.A.M. Yassin, 2009. Strontium sulphate scale formation in oil reservoir during water injection at high-salinity formation water. *Asian J. Applied Sci.*, 2: 300-317.
- Mohaghegh, S., B. Balan and S. Ameri, 1995. State-of-the-art in permeability determination from well log data: Part 2-verifiable, accurate permeability predictions, the touch-stone of all models. Proceedings of the SPE Eastern Regional Conference and Exhibition, September 17-21, 1995, Morgantown, West Virginia, pp: 1-5.
- Mohaghegh, S., B. Balan and S. Ameri, 1997. Permeability determination from well log data. Proceedings of the 1995 SPE Eastern Regional Conference and Exhibition, September 19-21, 1995, Morgantown, West Virginia, pp: 170-174.
- Morrow, C., D. Lockner, S. Hickman, M. Rusanov and T. Roedel, 1994. Effects of lithology and depth on the permeability of core samples from the Kola and KTB drill holes. *J. Geophys. Res.*, 99: 7263-7274.
- NIH, 1998. Spatial variability of groundwater quality in Jammu District (J and K). National Institute of Hydrology, CS (AR)-25/98-99, http://nih.ernet.in/TechnicalPapers/Spatial_Variability_of_Ground_Water_Quality_in_Jammu_District.pdf
- Negreiros, J., M. Painho, F. Aguilar and M. Aguilar, 2010. Geographical information systems principles of ordinary kriging interpolator. *J. Applied Sci.*, 10: 852-867.
- Orodu, O.D., Z. Tang and Q. Fei, 2009. Hydraulic (Flow) unit determination and permeability prediction: A case study of block Shen-95, Liaohe oilfield, North-East China. *J. Applied Sci.*, 10: 1801-1816.
- Qobi, L., A. de Kuijper, X.M. Tang and J. Strauss, 2001. Permeability determination from Stoneley waves in the Ara group carbonates, Oman. *GeoArabia*, 6: 649-666.

- Rabah, F.K.J., S.M. Ghabayen and A.A. Salha, 2011. Effect of GIS interpolation techniques on the accuracy of the spatial representation of groundwater monitoring data in Gaza strip. *J. Environ. Sci. Technol.*, 4: 579-589.
- Saar, M.O. and M. Manga, 2004. Depth dependence of permeability in the Oregon Cascades inferred from hydrogeologic, thermal, seismic and magmatic modeling constraints. *J. Geophys. Res.*, Vol. 109, 10.1029/2003JB002855.
- Shang, B.Z., J.G. Hamman, H. Chen and D.H. Caldwell, 2003. A model to correlate permeability with efficient porosity and irreducible water saturation. Proceedings of the SPE Annual Technical Conference and Exhibition, 5-8 October, 2003, Denver, Colorado.
- Sokouti, R. and M.H. Mahdian, 2009. Comparative efficacy of some geostatistical methods for the estimation of spatial variability of topsoil salinity. *J. Applied Sci.*, 9: 588-592.
- Tang, X. and C.H. Cheng, 1996. Fast inversion of formation permeability from Stoneley wave logs using a simplified Biot-Rosenbaum model. *Geophysics*, 61: 639-645.
- Todd, K.D., 2004. *Groundwater Hydrology*. 2nd Edn., John Wiley and Sons, New York, pp: 65.
- Tonkin, M.J. and S.P. Larson, 2002. Kriging water levels with a regional-linear and point-logarithmic drift. *Ground Water*, 40: 185-193.
- Vann, J., S. Jackson and O. Bertoli, 2003. Quantitative kriging neighbourhood analysis for the mining geologist-a description of the method with worked case examples. Proceedings of the 5th International Mining Geology Conference, November 17-19, 2003, Bendigo, Victoria.
- Yamamoto, T., 2003. Imaging permeability structure within the highly permeable carbonate earth: Inverse theory and experiment. *Geophysics*, 68: 1189-1201.
- Yasrebi, J., M. Saffari, H. Fathi, N. Karimian, M. Emadi and M. Baghernejad, 2008. Spatial variability of soil fertility properties for precision agriculture in Southern Iran. *J. Applied Sci.*, 8: 1642-1650.